AIP | APL Materials

Bi-alkali antimonide photocathodes for high brightness accelerators

S. Schubert, M. Ruiz-Osés, I. Ben-Zvi, T. Kamps, X. Liang, E. Muller, K. Müller, H. Padmore, T. Rao, X. Tong, T. Vecchione, and J. Smedley

Citation: APL Mater. **1**, 032119 (2013); doi: 10.1063/1.4821625
View online: http://dx.doi.org/10.1063/1.4821625
View Table of Contents: http://scitation.aip.org/content/aip/journal/aplmater/1/3?ver=pdfcov
Published by the AIP Publishing

APL MATERIALS 1, 032119 (2013)

Bi-alkali antimonide photocathodes for high brightness accelerators

S. Schubert,[1,2] M. Ruiz-Osés,[3] I. Ben-Zvi,[3] T. Kamps,[1] X. Liang,[3]
E. Muller,[2] K. Müller,[4,a] H. Padmore,[5] T. Rao,[2] X. Tong,[4]
T. Vecchione,[5,b] and J. Smedley[2,c]
[1]*Helmholtz-Zentrum Berlin, 12489 Berlin, Germany*
[2]*Brookhaven National Laboratory, Upton, New York 11973, USA*
[3]*Stony Brook University, Stony Brook, New York 11794, USA*
[4]*Center for Functional Nanomaterials, BNL, Upton, New York 11973, USA*
[5]*Lawrence Berkeley National Laboratory, Berkeley, California 94720, USA*

(Received 28 May 2013; accepted 18 July 2013; published online 20 September 2013)

Alkali-antimonide photocathodes were grown on Si(100) and studied by means of XPS and UHV-AFM to validate the growth procedure and morphology of this material. The elements were evaporated sequentially at elevated substrate temperatures (first Sb, second K, third Cs). The generated intermediate K-Sb compound itself is a photocathode and the composition of $K_{2.4}Sb$ is close to the favored K_3Sb stoichiometry. After cesium deposition, the surface layer is cesium enriched. The determined rms roughness of 25 nm results in a roughness domination of the emittance in the photoinjector already above 3 MV/m. [http://dx.doi.org/10.1063/1.4821625]

Since the 1960s, multi-alkali antimonide photocathodes are a continuous field of research in the photomultiplier tube area. These materials are favored for their high quantum efficiency in the visible region and therefore used in a wide range of photon detector devices.[1] They are also of great interest for the particle accelerator community. Future particle sources call for an electron emitting material with a high quantum efficiency in the visible part of the spectrum preferably in the green to match the drive laser wavelength, short response time, low dark current, and the ability to produce high-brightness beams with a relatively low emittance.[2–4] Still the alkali-antimonide photocathodes have been grown by traditional recipes with only passing interest in the solid state chemistry of the formation process.[5–8] Today's material science techniques provide manifold methods to measure and probe the materials composition and behavior. Our goal was to identify the chemical composition and surface morphology of the compounds involved in the cesium-potassium-antimonide photocathode production following the growth procedure described by Sommer.[8] We used core-level x-ray photoelectron spectroscopy (XPS) to reveal the chemical composition and oxidation state of the components in the critical near surface region after each growth step and an UHV-atomic force microscope (UHV-AFM) for roughness determination and surface morphology, which has been demonstrated to be critical to the emittance performance of these cathodes.[9] The results of these measurements will be compared with previously performed X-ray diffraction measurements.[10]

XPS and UHV-AFM experiments were carried out at the Center of Functional Nanomaterials (CFN) at Brookhaven National Laboratory (BNL). The UHV chamber for this measurements with a base pressure of 3×10^{-10} Torr is equipped with an x-ray photoelectron spectrometer (Specs Phoibos 100 MCD analyzer) and a commercial RHK UHV-750 variable temperature scanning-tunneling and

[a]Present address: Zernike Institute for Advanced Materials, University of Groningen, Netherlands
[b]Present address: SLAC National Accelerator Laboratory, Menlo Park, California 94025-7015, USA
[c]Author to whom correspondence should be addressed. Electronic mail: smedley@bnl.gov

atomic force microscope (STM/AFM). Al-Kα X-ray radiation (1486 eV photon energy) was used for the XPS studies. The measurements were taken in the constant analyzer energy mode (CAE) at 20 eV pass energy, the later given binding energies are with 0.25 eV resolution. AFM images were obtained in contact mode with a silicon cantilever. Evaporation rates were monitored with a quartz-micro balance. The photo-current was produced by means of a III-class green laser of 532 nm and 6 mW, a negative bias of −10 V was applied to the sample. All given values for quantum efficiency are for excitation with a 532 nm wavelength laser.

Atomically flat Si(100) p-type wafers were used as substrates, the wafers were HF dipped, rinsed with deionized water and dried prior to mounting inside the vacuum chamber to ensure cleanliness of the substrate surface and to remove the oxide layer. During mounting the substrate was exposed to air and therefore, was heated to 100 °C in UHV for degassing. The antimony layer was grown either by evaporation at 100 °C substrate temperature or sputter deposited at room temperature in a Kurt Lesker LAB 18 modular PVD system. Sputtered films usually showed a large amount of oxidized Antimony. For 5 nm antimony films, we were able to remove most of the oxide by heating to 400 °C for about 4 min, for further details see Ref. 11.

The alkali-metals were evaporated from commercial alvatec sources. Usually during evaporation the pressure in the chamber did not exceed 2×10^{-9} Torr. After the antimony, the alkalis were evaporated in sequence, following the recipe from Sommer.[8] Potassium was evaporated with a constant rate of 0.2 Å/s. The substrate temperature was held at 135 °C. During growth the photo-current was monitored. A constant flux of potassium was offered to the surface as long as the quantum efficiency increased. Then evaporation was stopped to record the photoelectron emission spectrum and investigate the composition of the intermediate compound. In some cases, the growth process was directly continued with cesium to decrease the oxygen uptake of the material during the time of the measurements. Cesium was deposited at or below 135 °C substrate temperature at an evaporation rate of 0.2 Å/s. The evaporation was stopped when the quantum efficiency reached a plateau. Cathodes produced with the above described procedure usually showed a quantum efficiency of 4%–6% in our homemade experimental setup,[10] while in the CFN user facility these values were slightly lower, 1%–2.5% which might be due to higher partial pressures of Water and other contaminants.

XPS was used to determine the surface layer composition. The escape depth for photoelectrons is less than 10 nm from the surface and this area is therefore referred to as surface layer. For evaluation of the chemical composition we considered the following regions (B.E.): Sb 3d/O 1s (542-520 eV), Cs 3d (775-705 eV), K 2p (320-275 eV), Si 2p (110-92 eV), survey spectra were taken after each deposition step before the region spectra. To obtain the chemical composition, the intensities obtained from the XPS fitting procedure were corrected by the corresponding atomic sensitivity factors. For this study atomic sensitivity factors from Ref. 12 were used. The values given are within an accuracy of 10%.

The CsK_2Sb photocathode was formed following the photomultiplier tube (PMT) recipe described by Sommer.[8] Unlike Sommer, who used glass as a substrate, the compound was grown on Si(100). The growth procedure started with the deposition of a 10–20 nm antimony layer at 100 °C substrate temperature. For the potassium and cesium deposition, the sample temperature was increased to 135 °C. The alkali were deposited seq\uentially, starting with potassium.

Antimony layer: Due to the mounting in air all substrates showed residual oxygen contamination, with an oxygen 1s signal around 532.7 eV. As a first growth step, antimony was deposited onto the Si(100) sample. Usually upon antimony evaporation, with a final thickness in the range of 10–20 nm, the oxygen and silicon signal could not be detected, see Figure 1(a). The deposited antimony usually showed Sb $3d_{3/2}$ and $3d_{5/2}$ peaks at 537.4 eV and 528.1 eV, respectively, for metallic antimony. From literature it is known that metallic antimony $3d_{3/2}$ and $3d_{5/2}$ binding energies are expected at 537.7 and 528.2 eV, respectively.[13] All studied Sb films exhibit 3d binding energies in good agreement with these numbers, indicating that the antimony layers were metallic. Amorphous layers would result in Sb 3d B.E. at higher energies, around 529.3 and 538.7 eV, respectively.[14] This finding is in good agreement with our XRD measurements which show that an amorphous to crystalline transition takes place around 7–8 nm film thickness.[11] The resultant spin orbit splitting for the metallic Sb 3d

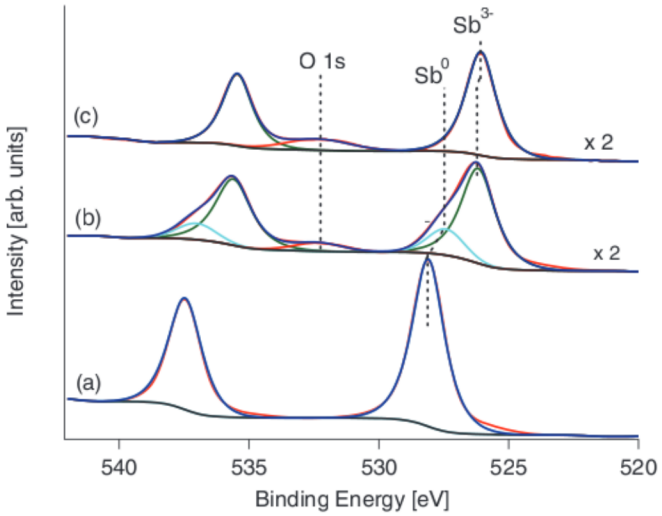

FIG. 1. XPS Sb 3d spectra; (a) after Sb deposition on Si(100); (b) after Potassium deposition; (c) after Cesium deposition; spectra b and c show traces of oxygen with a peak maximum around 532.3 eV.

was found to be 9.4 eV and the intensity ratio $3d_{3/2}$:$3d_{5/2}$ = 0.67 is in good agreement with values found in the literature.[15] Cathodes grown from sputter deposited Sb films, which under went the heating cycle described before, yield the same results in terms of XPS and quantum efficiency as cathodes grown from evaporated Sb films.

Potassium-antimony layer: Following the PMT technology of growth,[8] as a second step potassium was evaporated on top of the previously evaporated or sputtered film of antimony. The deposition was stopped once a plateau in photocurrent was recorded. After deposition most of the preadsorbed antimony reacted with potassium, the final mixture showed a composition of $K_{2.4}$ Sb. The stoichiometric ratio of 2.4:1 is due to a mixture of K_3Sb and other KSb compounds in the surface layer. The antimony spectra, Figure 1(b), showed contributions of elemental and reduced antimony, peaks were found at 3d (537.1 eV and 527.5 eV) and (535.4 eV and 526.2 eV), respectively. The potassium $2p_{1/2}$ and $2p_{3/2}$ peaks appeared at 296.2 eV and 293.4 eV, respectively, with a spin-orbit splitting of 2.8 eV and an intensity ratio of 2 $p_{1/2}$:$2p_{3/2}$=0.5, see Figure 2(a). These values are in good agreement with potassium core level values found in the literature for potassium-antimonides.[15] The binding energy values are shifted by 1.4 eV to lower binding energies with respect to the expected metallic potassium 2p core levels.[16]

The K-Sb phase is an intermediate step in the CsK_2Sb growth, previously it was believed that this intermediate step consisted solely of K_3Sb.[15,17] Although the intermediate phase is predominantly K_3Sb our combined XPS and XRD experiments show that small amounts other K-Sb phases are also present.[10] This phase usually showed a quantum efficiency of 0.1% to 0.2%.

Cesium-potassium-antimony layer: After the potassium deposition cesium was evaporated at elevated substrate temperatures (135 °C) until again a plateau in the photocurrent was reached. The evaluated cathodes showed a quantum efficiency around 1%–2.5%. The cesium $3d_{3/2}$ and $3d_{5/2}$ peaks are found at 739.1 eV and 725.3 eV, respectively, the resultant spin-orbit splitting is 13.8 eV. Similar binding energies for the Cs^+ 3d core levels were determined by Soriano in alkali-antimonide compounds[15] and Yang and Ebbinghaus for Cs_2O.[18,19] The Cs 3d signals in our samples were always symmetric and sharp with FWHM around 2 eV, it can be concluded that cesium was not present in a cluster-like environment but segregated into the K-Sb structure.[19] In comparison to the K-Sb compound, the potassium 2p core levels are shifted by approx. 0.2 eV towards lower binding energies in the Cs-K-Sb samples, see Figure 2(b). This shift might be due to a transition from n-type K_3Sb to a p-type CsKSb compound.[20] The final composition of the photocathodes was determined to be $Cs_{2.1}K_{1.1}Sb$. Cesium enrichment was also found by others.[15,21] Valeri *et al.* ascribed it to potassium

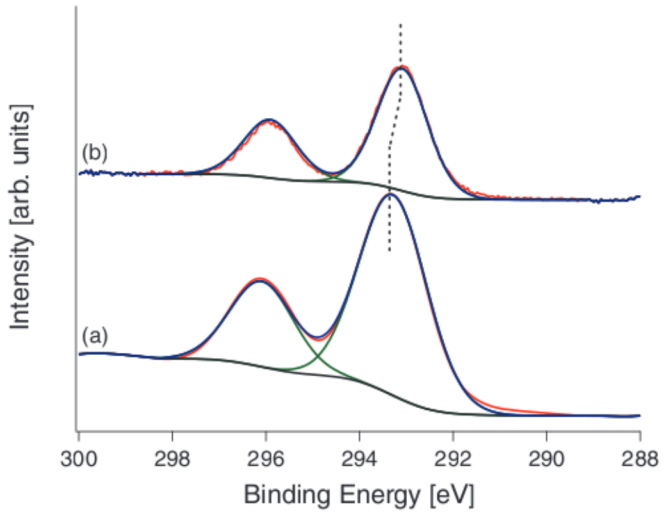

FIG. 2. XPS K 2p spectra; (a) after K deposition on Si(100); (b) after Cesium deposition.

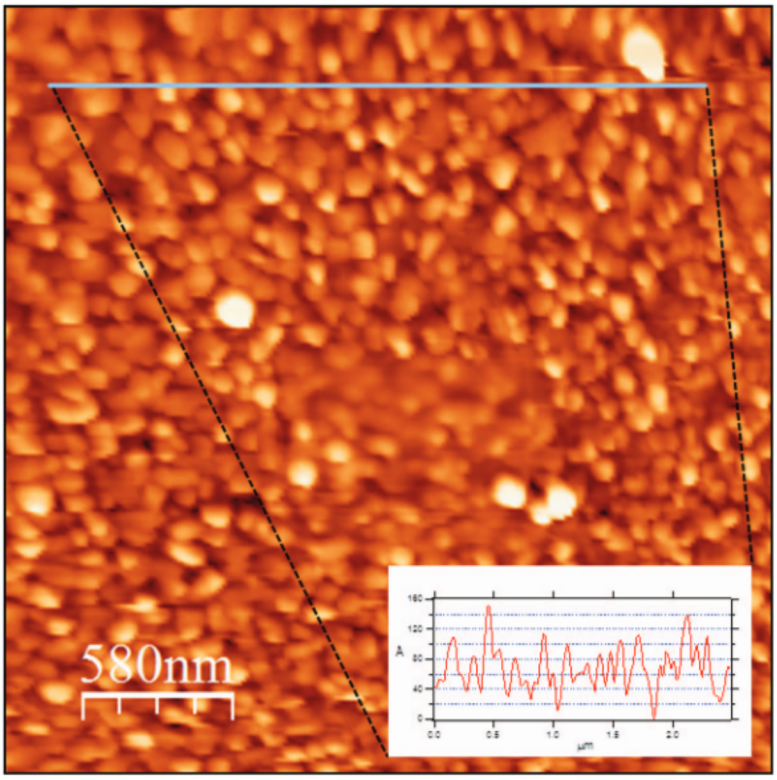

FIG. 3. AFM topography image (3 μm × 3 μm) and line profile for a Cs-K-Sb photocathode with 1.1% q.e.

segregation into the bulk due to surface oxygen.[21] This cannot be totally excluded in the presented case, since the Si surface showed oxygen contamination, as well as an oxygen contribution is visible in the final cathode material, see Figure 1(c). On the other hand in the similar system of the Na_2KSb photocathode a potassium enriched surface layer (NaK_2Sb) over a alkali deficient bulk is found.[22] In this case, the reversed alkali ratio in the surface is ascribed to diffusion of potassium from the bulk to the surface and might very well be also true for the presented case of the CsK_2Sb photocathode.

After the growth procedure, we performed UHV-AFM measurements, see Figure 3. From these measurements, we cannot only picture the surface morphology but also the root mean square (rms)

roughness of the surface. This information is crucial since from the roughness the cathode emittance contribution can be predicted.[9] Figure 3(a) shows an AFM topography image of a full photocathode with a quantum efficiency of 1.1%. The material grows in pillars with a 100 nm spatial period. The rms roughness was determined to be about 25 nm. Using the equation from Ref. 9 which describes the field and roughness dependence of the emittance, it was found that above 3 MV/m the roughness is the dominant effect on the emittance and is about 1 μm/mm at 20 MV/m accelerating field.

Cs-K-Sb photocathodes were studied by means of XPS and UHV-AFM during growth. XPS showed that the surface of the grown cathodes consists of a cesium enriched phase, whereas XRD measurements show CsK_2Sb composition of the bulk.[10] The cesium enrichment on the surface might be favorable in terms of band bending and final quantum efficiency of the photocathode and needs to be further investigated. Rms roughness, being one of the main parameters which influence the photocathode performance in the electron injector, needs to be as low as possible. Therefore, a roughness domination of the emittance above 3 MV/m accelerating field is not tolerable in future photoinjector operation. Therefore, possibilities to decrease the surface roughness need to be explored.

Research carried out in whole at the Center for Functional Nanomaterials, Brookhaven National Laboratory, which is supported by the U.S. Department of Energy, Office of Basic Energy Sciences, under Contract No. DE-AC02-98CH10886. Funding was received from the U.S. Department of Energy (DOE) under Grant Nos. KC-04-01-010 and DE-FG02-12ER41837 and the Bundesministerium fuer Bildung und Forschung (BMBF) and the Land Berlin, Germany.

[1] A. H. Sommer, "Multi-alkali photocathodes," IRE Trans. Nucl. Sci. **3**, 8–12 (1956).
[2] D. H. Dowell, I. Bazarov, B. Dunham, K. Harkay, C. Hernandez-Garcia, R. Legg, H. Padmore, T. Rao, J. Smedley, and W. Wan, "Cathode R and D for future light sources," Nucl. Instrum. Methods Phys. Res. A **622**, 685–697 (2010).
[3] T. Rao, A. Burrill, X. Y. Chang, J. Smedley, T. Nishitani, C. Hernandez-Garcia, M. Poelker, E. Seddon, F. E. Hannon, C. K. Sinclair, J. Lewelle, and D. Feldman, "Photocathodes for the energy recovery linac," Nucl. Instrum. Methods Phys. Res. A **557**, 124–130 (2006).
[4] R. R. Mammei, R. Suleiman, J. Feingold, P. A. Adderley, J. Clark, S. Covert, J. Grames, J. Hansknecht, D. Machie, M. Poelker, T. Rao, J. Smedley, J. Walsh, J. L. McCarter, and M. Ruiz-Osés, "Charge lifetime measurements at high average current using a K_2CsSb photocathode inside a dc high voltage photogun," Phys. Rev. ST Accel. Beams **16**, 033401 (2013).
[5] M. C. McCarroll, R. J. Paff, and A. H. Sommer, "Role of Cs in (Cs) Na_2KSb (S20) multialkali photocathode," J. Appl. Phys. **42**, 569–572 (1971).
[6] C. Ghosh and B. P. Varma, "Preparation and study of properties of a few Alkali antimonide photocathodes," J. Appl. Phys. **49**, 4549–4553 (1978).
[7] C. W. Bates, D. D. Gupta, L. Galan, and D. N. E. Buchanan, "X-ray photoemission studies of cesium antimonide photoemitters," Thin Solid Films **69**, 175–182 (1980).
[8] A. H. Sommer, *Photoemissive Materials: Preparation , Properties and Use* (John Wiley & Sons Inc., 1969).
[9] T. Vecchione, J. Feng, H. A. Padmore, I. Ben-Zvi, X. Liang, M. Ruiz-Osés, T. Rao, J. Smedley, and D. Dowel, "Effect of roughness on emittance of potassium cesium antimonide photocathodes," in *Proceedings of the 2012 International Accelerator Conference* (IPAC12 OC, 2012), paper MOPPP041, pp. 655–657.
[10] M. Ruiz-Osés *et al.*, "*In-situ* x-ray diffraction characterization of bi-alkali antimonide photocathodes for high brightness accelerators" (unpublished).
[11] M. Ruiz-Osés *et al.*, "Antimony Surface Preparation for Alkali Antimonide Photocathodes" (unpublished).
[12] C. D. Wagner, L. E. Davis, M. V. Zeller, J. A. Taylor, R. M. Raymond, and L. H. Gale, "Empirical atomic sensitivity factors for qualitative analysis by electron spectroscopy for chemical analysis," Surf. Interface Anal. **3**, 211 (1981).
[13] M. Cordona and L. Ley, "Photoemission in solids i," Top. Appl. Phys. **26**, 271 (1978).
[14] C. W. Bates, Th. M. van Atekum, G. K. Wertheim, D. N. E. Buchanan, and K. E. Clements, "X-ray photoemission studies of superficially oxidized cesium antimonide photoemitters," Appl. Phys. Lett. **38**, 387–389 (1981).
[15] L. Soriano and L. Galán, "Interaction of cesium-potassium antimonide photocathode materials with oxygen: An x-ray photoelectron spectroscopy study," Jpn. J. Appl. Phys. **32**, 4737–4744 (1993).
[16] L.-G. Petersson and S.-E. Karlsson, "Clean and oxygen exposed potassium studied by photoelectron spectroscopy," Phys. Scr. **16**, 425–431 (1977).
[17] A. Braem, C. Joram, F. Piuz, E. Schyns, and J. Séguinot, "Technology of photocathode production," Nucl. Instrum. Methods Phys. Res. A **502**, 205–210 (2003).
[18] S.-J. Yang and C. W. Bates, Jr., "The role of cesium suboxides in low-work-function surface layers studied by x-ray photoelectron spectroscopy: Ag-O-Cs," Appl. Phys. Lett. **36**, 675–677 (1980).

[19] G. Ebbinghaus and A. Simon, "Electronic structure of Rb, Cs and some of their metallic oxides studied by photoelectron spectroscopy," Chem. Phys. **43**, 117–133 (1979).
[20] S. Imamura, "Electrical properties of alkali-antimonides," J. Phys. Soc. Jpn. **14**, 1491–1496 (1959).
[21] S. Valeri, G. Lancellotti, A. di Bona, U. del Pennino, C. Mariani, M. Sancrotti, C. Pagani, and P. Michelato, "Spectroscopic investigation of *in-situ* prepared multialkali-based photocathodes," in *Proceedings of the European Particle Accelerator Conference (EPAC-94)* (London, 1994), Vol. 94, p. 1459.
[22] L. Galan and C. W. Bates, "Structure of multialkali antimonide photocathodes studied by x-ray photoelectron spectroscopy," J. Phys. D **14**, 293–299 (1981).